

---

# Deep Spiking Networks

---

**Peter O'Connor**

QUVA Lab, Science Park 904, 1098 XH Amsterdam

**Max Welling**

QUVA Lab, Science Park 904, 1098 XH Amsterdam

P.E.OCONNOR@UVA.NL

M.WELLING@UVA.NL

## Abstract

We introduce the Spiking Multi-Layer Perceptron (SMLP). The SMLP is a spiking version of a conventional Multi-Layer Perceptron with rectified-linear units. Our architecture is event-based, meaning that neurons in the network communicate by sending “events” to downstream neurons, and that the state of each neuron is only updated when it receives an event. We show that the SMLP behaves identically, during both prediction and training, to a conventional deep network of rectified-linear units in the limiting case where we run the spiking network for a long time. We apply this architecture to a conventional classification problem (MNIST) and achieve performance very close to that of a conventional MLP with the same architecture. Our network is a natural architecture for learning based on streaming event-based data, and has potential applications in robotic systems, which require low power and low response latency.

## 1. Introduction

In recent years the success of Deep Learning has proven that a lot of problems in machine-learning can be successfully attacked by applying backpropagation to learn multiple layers of representation. Most of the recent breakthroughs have been achieved through purely supervised learning.

In the standard application of a deep network to a supervised-learning task, we feed some input vector through multiple hidden layers to produce a prediction, which is in turn compared to some target value to find a scalar cost. Parameters of the network are then updated according to their derivatives with respect to that cost. This

---

*Proceedings of the 33<sup>rd</sup> International Conference on Machine Learning*, New York, NY, USA, 2016. JMLR: W&CP volume 48. Copyright 2016 by the author(s).

approach requires that all modules within the network be differentiable. If they are not, no gradient can flow through them, and backpropagation will therefore not work.

An alternative class of artificial neural networks are Spiking Neural Networks. These networks, inspired by biology, consist of neurons that have some persistent “potential” which we refer to as  $\phi$ , and alter each-others’ potentials by sending “spikes” to one another. When unit  $i$  sends a spike, it increments the potential of each downstream unit  $j$  in proportion to the synaptic weight  $W_{i,j}$  connecting the units. If this increment brings unit  $j$ ’s potential past some threshold, unit  $j$  will send a spike to its downstream units.

One way to implement a spiking network is as an “event-based” system. In an event-based neural network, the state of unit  $j$  is only recomputed when it receives a spike from unit  $i$ . Such systems therefore have the interesting property that the amount of computation done depends on the contents of the data, since a neuron may be tuned to produce more spikes in response to some pattern of inputs than another.

An advantage of event-based neural networks is that a given update requires little computation. If an input spike, on average, causes one spike in each downstream layer of the network, the average cost will be  $\mathcal{O}(\sum_{l=1}^L N_l)$ , where  $N_l$  is the number of units in the layer  $l$ . Compare this to a standard network, where the basic messaging entity is a vector. When a vector arrives at the input, the cost of update will be  $\mathcal{O}(\sum_{l=1}^L (N_{l-1} \cdot N_l))$ . Event-based approaches are therefore interesting in real-time applications, wherein a single spike may carry an important piece of information that must be processed quickly and will therefore require low-latency.

Event based networks are well-adapted to handle data from event-based sensors, such as the Dynamic Vision Sensor (a.k.a. Silicon Retina, a vision sensor) (Lichtsteiner et al., 2008) and the Silicon Cochlea (an audio sensor) (Chan et al., 2007). Instead of sending out samples at a regular rate, as most sensors do, these sensors asynchronously out-

put events when there is a change in the input. They can thus react with very low latency to sensory events, and produce very sparse data. These events could be directly fed into our spiking network (whereas they would have to be binned over time and turned into a vector to be used with a conventional deep network).

The remainder of this paper is structured as follows: In Section 2 we discuss past work in combining spiking neural networks and deep learning. In 3 we describe our Spiking Multi-Layer Perceptron. In 4 we show experimental results demonstrating that our network behaves similarly to a conventional deep network in a classification setting. In 5 we discuss the implications of this research and our next steps.

## 2. Related Work

There has been little work on combining the fields of Deep Learning and Spiking neural networks. The main reason for this is that there is not an obvious way to backpropagate an error signal through a spiking network, since output consist of discrete events, rather than smoothly differentiable functions of the input. (Bohte et al., 2000) proposes a spiking deep learning algorithm - but it involves simulating a dynamical system, is specific to learning temporal spike patterns, and has not yet been applied at any scale. (Buesing et al., 2011) shows how a somewhat biologically plausible spiking network can be interpreted as an MCMC sampler of a high-dimensional probability distribution. (Diehl et al.) does classification on MNIST with a deep event-based network, but training is done with a regular deep network which is then converted to the spiking domain. A similar approach was used by (Hunsberger and Eliasmith, 2015) - they came up with a continuous unit which smoothly approximated the the firing rate of a spiking neuron, and did backpropagation on that, then transferred the learned parameters to a spiking network. (Neftci et al., 2013) came up with an event-based version of the contrastive-divergence algorithm, which can be used to train a Restricted Boltzmann Machine, but it was never applied in a Deep-Belief Net to learn multiple layers of representation. (O’Connor et al., 2013) did create an event-based spiking Deep Belief Net and fed it inputs from event-based sensors, but the network was trained offline in a vector-based system before being converted to run as a spiking network.

This paper introduces the first multi-layer network that is both trained and tested as a spiking network, and is applicable to arbitrary data. Our architecture is event based, and under certain configurations it requires no multiplication and only integer addition, which potentially makes it very amenable to efficient hardware implementation. We believe that this will help pave the way to on-line deep learning in real-time systems.

## 3. Methods

In Sections 3.1-3.4 we describe the components used in our model. In Section 3.5 we will use these components to put together a Spiking Multi-Layer Perceptron.

### 3.1. Variable-Spike Quantization

The units in our network use an algorithm that we refer to as Variable-Spike Quantization to generate events.

Take a real vector:  $\vec{v}$ . We can approximate this vector by a series of "signed spikes":

$$\vec{v} \approx \frac{1}{T} \sum_{n=1}^N e_{i_n}^{\vec{s}} s_n \quad (1)$$

where  $T$  represents the total number of time bins,  $e_{i_n}^{\vec{s}}$  is an one-hot encoded vector with index  $i_n$  set to 1,  $i_n$  is the index of the unit from which the  $n$ 'th spike fires (note that zero or multiple spikes can fire within one time bin),  $s_n \in \{-1, +1\}$  is the sign of the  $n$ 'th spike. These quantities are determined by Algorithm 1. In this procedure, we maintain an internal state vector  $\vec{\phi}$ . Every time we emit a spike we decrement  $\vec{\phi}$  until it is in the box bounded by  $(-\frac{1}{2}, \frac{1}{2}), (-\frac{1}{2}, \frac{1}{2})$

---

**Algorithm 1** Drawing a sequence of signed-spikes from a vector. The same function can be implemented much more efficiently using a Priority Queue - This implementation is for clarity. Note that if one does not care about the order of events within a single time step  $t$ , this function could be implemented in parallel with each unit simply emitting an event and decrementing it's  $\phi_i$  by  $s$  until its  $|\phi_i|$  is below  $\frac{1}{2}$ .

---

```

1: Input: vector  $v$ , int  $T$ 
2: for  $t \in 1 \dots T$  do
3:    $\vec{\phi} \leftarrow \vec{\phi} + \vec{v}$ 
4:   while True do
5:      $i \leftarrow \text{argmax}(|\vec{\phi}|)$ 
6:     if  $|\phi_i| > \frac{1}{2}$  then
7:        $s \leftarrow \text{sign}(\phi_i)$ 
8:        $\vec{\phi}_i \leftarrow \vec{\phi}_i - s$ 
9:       FireSignedSpike(source =  $i$ , sign =  $s$ )
10:    else
11:      break

```

---

Since  $\forall i : -\frac{1}{2} < \phi_i < \frac{1}{2}$  the L1 norm is bounded by:

$$\|\phi_T\|_{L1} = \left\| \sum_{t=1}^T v - \sum_{n=1}^N e_{i_n}^{\vec{s}} s_n \right\|_{L1} < \frac{l(\vec{v})}{2} \quad (2)$$

where  $l(\vec{v})$  is the number of elements in vector  $\vec{v}$ . We can

take the limit of infinite time, and show that our spikes converge to form an approximation of  $\vec{v}$ :

$$\begin{aligned} \lim_{T \rightarrow \infty} : \frac{1}{T} \|\phi_T\|_{L1} &= 0 \\ \lim_{T \rightarrow \infty} : \left\| \frac{1}{T} \sum_{t=1}^T v - \frac{1}{T} \sum_{n=1}^N e_{i_n}^{\vec{s}} s_n \right\|_{L1} &= 0 \\ \lim_{T \rightarrow \infty} : \vec{v} &= \frac{1}{T} \sum_{n=1}^N e_{i_n}^{\vec{s}} s_n \end{aligned} \quad (3)$$

Our algorithm is simply doing a discrete-time, bidirectional version of Delta-Sigma modulation - in which we encode floating point elements of our vector  $\vec{v}$  as a stream of signed events. We can view of this as doing a sort of ‘‘deterministic sampling’’ or ‘‘herding’’ (Welling, 2009) of the vector  $v$ . Figure 1 shows how the cumulative vector from our stream of events approaches the true value of  $v$  at a rate of  $1/T$ . We can compare this to another approach in which we stochastically sample spikes from the vector  $\vec{v}$ , as shown in Appendix A, which has a convergence of  $1/\sqrt{T}$ .

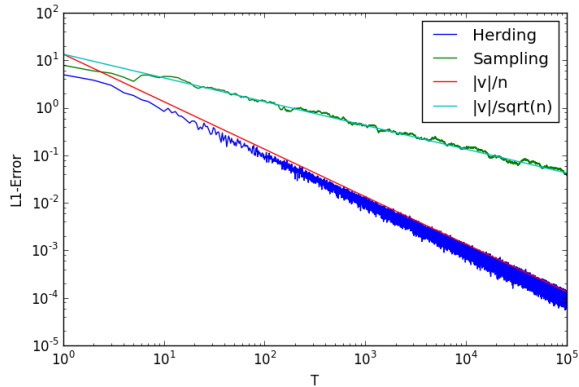


Figure 1: Variable-Spike Quantization shows  $1/T$  convergence, while ordinary sampling converges at a rate of  $1/\sqrt{T}$ . Note both x and y axes are log-scaled.

### 3.2. Quantizing Vector streams

A small modification to the above proof allows us to turn a stream of vectors into a stream of events.

If instead of a fixed vector  $\vec{v}$  we take a stream of vectors  $v_{stream} = \{v_1, \dots, v_T\}$ , we can modify the quantization algorithm (see QuantizeStream in Appendix A) to increment  $\phi$  by  $v_t$  on timestep  $t$ .

With a vector stream, Equation 3 is modified to:

$$\lim_{T \rightarrow \infty} : \frac{1}{T} \left\| \sum_{t=1}^T \vec{v}_t - \sum_{n=1}^N e_{i_n}^{\vec{s}} s_n \right\|_{L1} = 0 \quad (4)$$

$$\lim_{T \rightarrow \infty} : \frac{1}{T} \sum_{t=1}^T \vec{v}_t = \frac{1}{T} \sum_{n=1}^N e_{i_n}^{\vec{s}} s_n \quad (5)$$

So we end up approximating the running mean of  $v_{stream}$ .

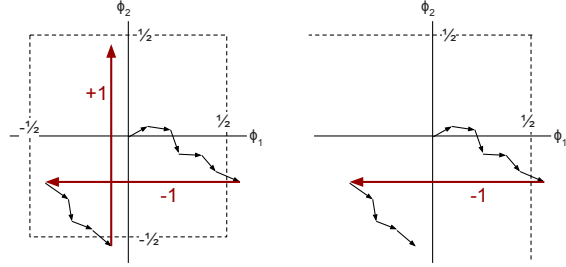


Figure 2: Left: An illustration of vector stream quantization (see QuantizeStream in Appendix A). Right: An illustration of vector-stream quantization and rectification (see Algorithm 2). The two axes represent the potentials  $\phi$  of each of two units in a layer. Black arrows represent successive input vectors  $v_T$ , and red arrows indicate the unit-decrement to  $\phi_i$  that happens when the threshold is crossed and a spike is emitted from unit  $i$ .

### 3.3. Incremental Dot-Product

Thus far, we’ve shown that our quantization method transforms a vector into a stream of events. Here we will show that this can be used to incrementally compute the dot product of a vector and a matrix. Suppose we define a vector

$$\vec{u} \leftarrow \vec{v} \cdot W \quad (6)$$

Where  $W$  is a matrix of parameters. If we extract a stream of events  $v_{stream}$  approximating  $\vec{v}$ , we can pass them through  $W$  to get a new stream of events that approximates  $\vec{u}$ :

$$\begin{aligned} \vec{u} &= \vec{v} \cdot W \\ &\approx \frac{1}{T} \left( \sum_{n=1}^N e_{i_n}^{\vec{s}} s_n \right) \cdot W \\ &= \frac{1}{T} \left( \sum_{n=1}^N s_n e_{i_n}^{\vec{s}} \cdot W \right) \\ &= \frac{1}{T} \left( \sum_{n=1}^N s_n \vec{W}_{i_n, \cdot} \right) \end{aligned} \quad (7)$$

Where  $W_{i, \cdot}$  is the  $i$ ’th row of matrix  $W$ .

### 3.4. Quantization and Rectification

We can modify our quantization algorithm to create an event-based version of a rectified-linear (ReLU) unit. To

---

**Algorithm 2** Drawing a sequence of positive spikes from a stream of vectors.

---

```

1: Input: List[Vector]: stream
2: for  $\vec{v}_t \in \text{stream}$  do
3:    $\vec{\phi} \leftarrow \vec{\phi} + \vec{v}_t$ 
4:   while True do
5:      $i \leftarrow \text{argmax}(\vec{\phi})$ 
6:     if  $\vec{\phi}_i > \frac{1}{2}$  then
7:        $\vec{\phi}_i \leftarrow \vec{\phi}_i - 1$ 
8:       FireSpike(source=i)
9:     else
10:      break

```

---

do this, we only fire events on positive threshold-crossings. This results in Algorithm 2.

It is not hard to see why this construction works. First observe that the total number of spikes emitted can be computed by considering the total cumulative sum  $\sum_{t=1}^T v_{j,t}$ . More precisely:

$$N_{j,T} = \max\left(0, \left\lfloor \max_{T' \in [1 \dots T]} \left( \sum_{t=1}^{T'} v_{j,t} + \frac{1}{2} \right) \right\rfloor\right) \quad (8)$$

where  $N_{j,T}$  indicates the number of spikes emitted from unit  $j$  by time  $T$  and  $\lfloor \cdot \rfloor$  indicates the integer floor of a real number.

Assume the  $v_{j,t}$  are IID sampled from some process with mean  $E[v_{j,t}] = \mu_j$  and finite standard deviation  $\sigma_j$ . Define  $\zeta_{j,t} = v_{j,t} - \mu_j$  which has zero mean and the cumulative sum  $\xi_{j,T} = \sum_{t=1}^T \zeta_{j,t}$  which is martingale. There are a number of concentration inequalities, such as the Bernstein concentration inequalities (Fan et al., 2012) that bound the sum or the maximum of the sequence  $\xi_{j,T}$  under various conditions. What is only important for us is the fact that in the limit  $T \rightarrow \infty$  the sums  $\xi_{j,T}$  concentrate to a delta peak at zero in probability and that we can therefore conclude  $\sum_{t=1}^T v_{j,t} \rightarrow T\mu_j$  from which we can also conclude that the maximum, and thus the number of spikes will grow in the same way. From this we finally conclude that  $\frac{N_{j,T}}{T} \rightarrow \max(0, \mu)$ , which is the ReLU non-linearity.

Thus the mean spiking rate approaches the ReLU function of the mean input. We will refer to our quantizing-rectifying module as a **quant-rect** module.

### 3.5. Constructing a Spiking Multi-Layer Perceptron

Using the parts we’ve described so far, we can construct a spiking MLP.

### 3.6. Forward Pass

The forward pass consists of alternating layers of weight modules and quant-rect modules (corresponding to the alternating weight-multiplications and rectifications in a traditional ReLU network. As the proofs so far have shown, the the overall function of the forward pass of the network should approach the function of the equivalent ReLU network as  $T \rightarrow \infty$ , since each component performs the equivalent function. Figure 4 demonstrates that our spiking network, if run for a long time, exactly approximates the behaviour of the ReLU network.

### 3.7. Backward Pass

In the backwards pass we propagate error spikes back so that their signals approximate the true gradients of the ReLU network. A ReLU unit has the function and derivative:

$$\begin{aligned} f(x) &= [x > 0] \cdot x \\ f'(x) &= [x > 0] \end{aligned} \quad (9)$$

Where:

$[x > 0]$  denotes a step function (1 if  $x > 0$  otherwise 0).

In the spiking domain, we express this simply by blocking error spikes on units for which the cumulative sum of inputs into that unit is below 0 (see the ”filter” modules in Figure 3).

The signed-spikes that come out of a layer’s filter module are used to index columns of that layer’s weight matrix, and negate them if the sign of the spike is negative. The resulting vector is then fed into the backwards quantization module, which in turn sends back error spikes to previous layers.

One problem we have is that, when errors are small, it is possible that the backwards quantizers never get a chance to emit a spike before the training round is over. If this is the case, we will never be able to learn once the magnitude of the error signal falls under a given threshold. Indeed, when initial weights are too low, and therefore the initial magnitude of the backpropagated error signal was too small, the network does not learn at all. This is not a problem in vector-based ReLU networks, because no matter how small the magnitude, some error signal will always get through (unless all hidden units are in their inactive regime) and the network will learn to increase the size of its weights.

In order to compensate for this, we found that a very effective solution is to uniformly randomize the initial  $\vec{\phi} \sim U(-\frac{1}{2}, \frac{1}{2})^D$  for each backwards-pass quantizer on each training iteration. This way, there is always some chance that an error signal will be sent. We found that this not only got us out of situations where we could not learn at all

## Spiking MLP

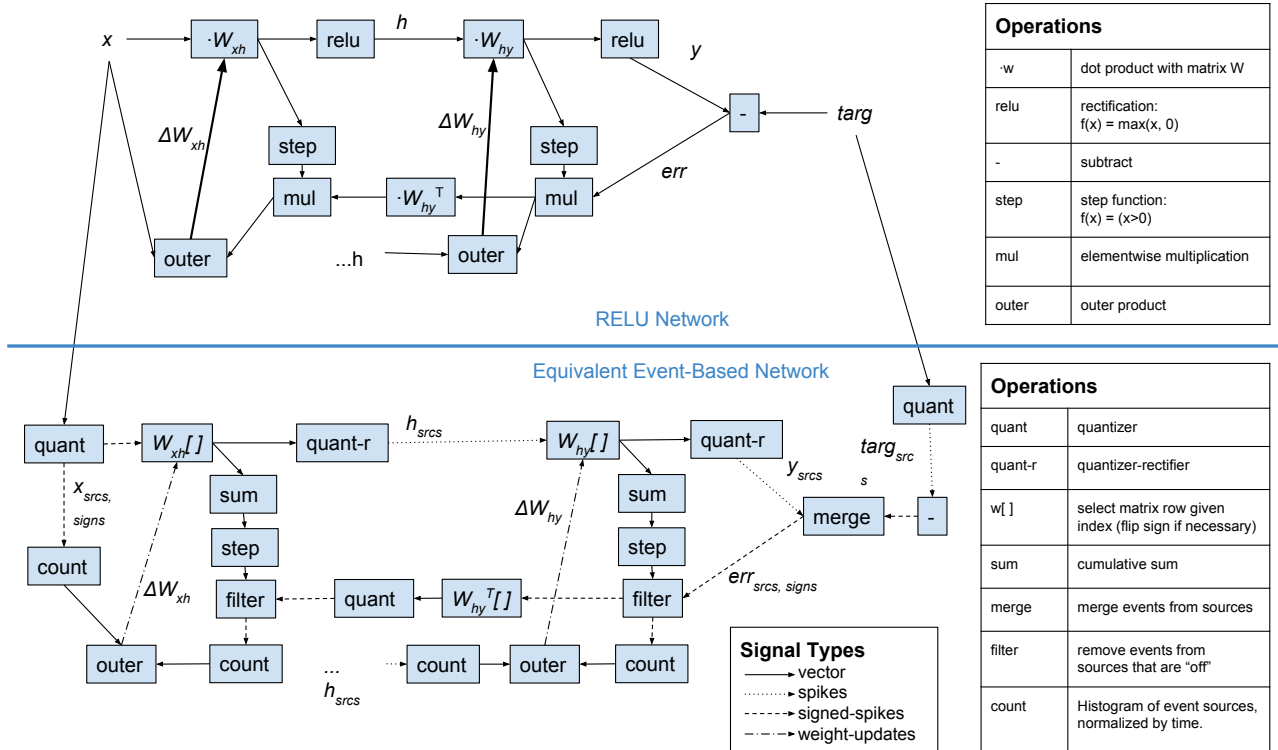


Figure 3: The architecture of the Spiking MLP. On the top, we have a conventional neural network of rectified linear units with one hidden layer. On the bottom, we have the equivalent spiking network.

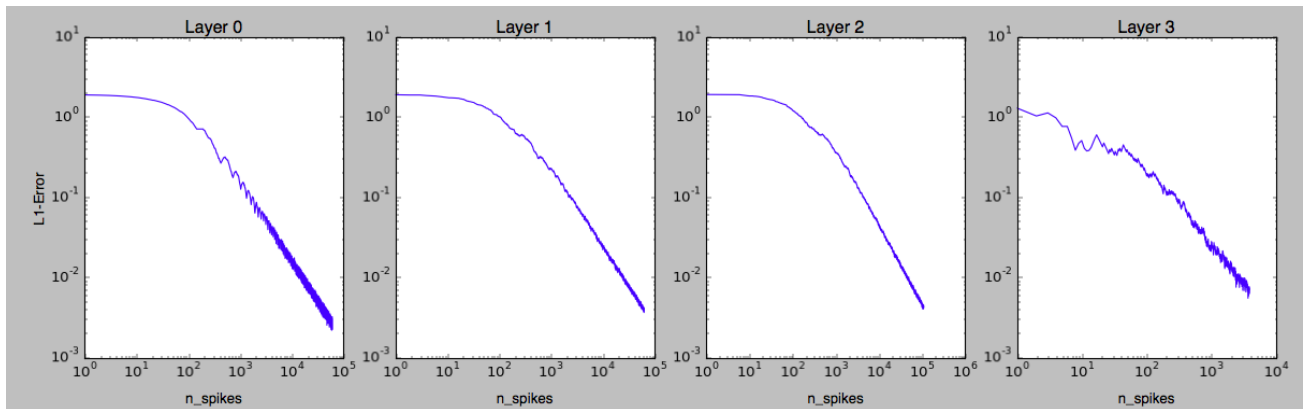


Figure 4: A 3-layer MLP (784-500-500-10) MLP with random weights ( $\sim \mathcal{N}(0, 0.1)$ ) is fed with a random input vector, and a forward pass is computed. We compare the response of the ReLU network to the counts of spikes from our spiking network, and see that over all layers, the responses converge as  $T \rightarrow \infty$ . Note both x and y axes are log-scaled.

due to small initial weights, but also improved our score on situations where we could learn.

A further issue that comes up when designing the backward pass is the order in which we process events. Since an event can activate a filter module which blocks the transmission of itself or future events on the backward pass, we need to think about the order in which we processing these events.

The topic of event-routing is explained in Appendix C.

### 3.8. Weight Updates

The “outer” modules in Figure 3 collect the input/error spike statistics, and feed changes back to the weight matrices. There are two methods by which we can update the weights. These are as follows:

**Fractional Stochastic Gradient Descent (FSGD)** Our spiking network introduces a new feature: if a data point is decomposed as a stream of events, we can do parameter updates even before a single data point has been observed, because with event-based processing, it is possible to send weight updates whenever an error event comes back. In this scheme, we send updates to a column of the weight matrix every time an error event comes in.

$$\Delta W_{:,i} \leftarrow -\frac{\eta}{T} \cdot s \cdot \vec{c}_{in} \quad (10)$$

Where  $\vec{c}_{in}$  is an integer vector of counted input spikes,  $\Delta W_{:,i}$  is the change to the  $i$ 'th column of the weight matrix,  $s \in \{-1, 1\}$  is the sign of the error event, and  $i$  is the index of the unit that produced that error event. This may help to avoid overshooting in learning. Since the value of the weight is now being updated with every new error event, fewer error events should be sent back once the weight matrix adjusts to correct the error.

**Stochastic Gradient Descent** We also have the option of sticking closer to the vector-based method. In this case, we collect two vectors,  $\vec{c}_{in}$  and  $\vec{c}_{out}$  and take their outer product at the end of a training iteration to compute the weight update:

$$\Delta W \leftarrow -\frac{\eta}{T} \cdot \vec{c}_{in} \otimes \vec{c}_{out} \quad (11)$$

### 3.9. Training

While the design of the network is suited for streaming temporal data, we can adapt it to be used in a more conventional classification setting. Here we will describe the approach we took.

We chose to train the network with 1 sample at a time, although in principle it is possible to do minibatch training. We select a number of time steps  $T$ , to run the network for each iteration of training. At the beginning of a round of training, we reset the network state (all  $\vec{\phi}$ 's and the state of the running sum modules). We also randomize the initial  $\vec{\phi}$  values of the modules in the backward-pass (as described in 3.7). On each time step  $t$ , we feed the input vector to the input quantizer (see Figure 3), and propagate the resulting spikes through the network. We then propagate an error spike back from the unit corresponding to the correct class label, and update the parameters by one of the two methods described in 3.8.

## 4. Experiments

### 4.1. Hyperparameters

Our spiking architecture introduced a number of new hyperparameters and settings that are unfamiliar with those

used to regular neural networks. We chose to evaluate these empirically by modifying them one-by-one as compared to a baseline.

- Fractional Updates.
  - False (Baseline): We use the standard stochastic-gradient descent method
  - True: We use our new Fractional Stochastic Gradient Descent method - described in section 3.8
- Depth-First
  - False (Baseline): Events are propagated "Breadth-first", meaning that, at a given time-step, all events are collected from the output of one module before any of their child-events are processed.
  - True: If an event from module A creates child-events from module B, those are processed immediately, before any more events from module A are processed.
- Smooth Weight Updates
  - False (Baseline): The weight-update modules take in a count of spikes from the previous layer as their input.
  - True: The weight-update modules take the rectified cumulative sum of the pre-quantized vectors from the previous layer - resulting in a smoother estimate of the input.
- Backwards-Quantization:
  - No-Reset-Quantization (Baseline): The backwards quantization modules do not reset their  $\vec{\phi}$ s with each training iteration.
  - Random: Each element of  $\vec{\phi}$  is randomly selection from the interval  $[-\frac{1}{2}, \frac{1}{2}]$  at the start of each training iteration.
  - Zero-Reset: The backwards quantizers reset their  $\vec{\phi}$ s to zero at the start of each training iteration.
- Number of time-steps: How many time steps to run the training procedure for each sample (Baseline is 10).

Since none of these hyperparameters have obvious values, we tested them empirically with a network with layer sizes [784-200-200-10], trained on MNIST. Table 1 shows the affects of these hyperparameters.

Table 1: Percent error on MNIST for various settings. We explore the effects of different network settings by changing one at a time, training on MNIST, and comparing the result to a baseline network. The baseline network has layer-sizes [784, 200, 200, 10], uses regular (non-fractional) stochastic gradient descent, uses Breadth-First (as opposed to Depth-First) event ordering, does not use smooth weight updates, uses the "No-reset" scheme for its backward pass quantizers, and runs for 10 time-steps on each iteration.

| Variant                        | % Error |
|--------------------------------|---------|
| Baseline                       | 3.38    |
| Fractional Updates             | 3.10    |
| Depth-First Propagation        | 81.47   |
| Smooth Gradients               | 2.85    |
| Smooth & Fractional            | 3.07    |
| Back-Quantization = Zero-Reset | 87.87   |
| Back-Quantization = Random     | 3.15    |
| 5 Time Steps                   | 4.41    |
| 20 Time Steps                  | 2.65    |

Most of the Hyperparameter settings appear to make a small difference. A notable exception is the Zero-Reset rule for our backwards-quantizing units - the network learns almost nothing throughout training. The reason for this is that the initial weights, which were drawn from  $\mathcal{N}(0, 0.01)$  are too small to allow any error-spikes to be sent back (the backward-pass quantizers never reach their firing thresholds). As a result, the network fails to learn. We found two ways to deal with this: "Back-Quantization = Random" initializes the  $\vec{\phi}$  for the backwards quantizers randomly at the beginning of each round of training. "Back-Quantization = No-Reset" simply does not reset  $\vec{\phi}$  in between training iterations. In both cases, the backwards pass quantizers always have some chance at sending a spike, and so the network is able to train. It is also interesting that using Fractional Updates (FSGD) gives us a slight advantage over regular SGD (Baseline). This is quite promising, because it means we have no need for multiplication in our network - As Section 3.8 explains, we simply add a column to the weight matrix every time an error spike arrives. We also observe that using the rectified running sum of the pre-quantization vector from the previous layer as our input to the weight-update module (Smooth Gradients) gives us a slight advantage. This is expected, because it is simply a less noisy version of the count of the input spikes that we would use otherwise.

#### 4.2. Comparison to ReLU Network

We ran both the spiking network and the equivalent ReLU network on MNIST, using an architecture with 2 fully-connected hidden layers, each consisting of 200 units. Re-

fer to Appendix B for a full description of hyperparameters.

| Network                   | % Test / Training Error |
|---------------------------|-------------------------|
| Vector ReLU MLP           | 1.81 / 0.23             |
| Spiking MLP               | 2.34 / 0.926            |
| Spiking with ReLU Weights | 1.92 / 0.254            |
| ReLU with Spiking weights | 2.20 / 0.878            |

Table 2: Scores of various implementations on MNIST after 20 epochs of training on a network with hidden layers of sizes [200, 200]. "Spiking with ReLU Weight" is the score if we set the parameters of the Spiking network to the already-trained parameters of the ReLU network, then use the Spiking Network to classify MNIST. "ReLU with Spiking weights" is the inverse - we take the parameters trained in the spiking network and map them to the ReLU net.

Table 2 shows the results of our experiment, after 20 epochs of training. We find that the Vector-based network does still outperform our spiking network, but only marginally. In order to determine how much of that difference was due to the fact that the Spiking network has a discrete forward pass, we mapped the learned parameters from the ReLU network onto the Spiking network, and used the Spiking network to classify - the performance of the spiking network improved nearly to that of the ReLU network (see "Spiking with ReLU Weights"), indicating that the difference was not just due to the discretization of the forward pass but also due to the parameters learned in training. We also did the inverse - mapped the parameters of the trained Spiking Net onto the ReLU net, and found that the performance became slightly worse than the original performance of the Spiking Network. This tells us that most of the difference in score is due to the approximations in training, rather than the forward pass.

Figure 5 shows the learning curves resulting from our training. The bottom subplot shows the mean number of spikes emitted per training iteration at various testing intervals. This ran somewhat contrary to our expectations. We expected the number of backpropagating error spikes (green line) to fall substantially over the course of training, as the network improved in its predictions, but we observe that the number of backpropagating error spikes decreases only mildly. Moreover, we see a slow and steady trend of increasing spike rates in the forward pass.

## 5. Discussion

We implemented a Spiking Multi-Layer Perceptron and showed that our network behaves very similarly to a conventional MLP with rectified-linear units. However, our model has some advantages over a regular MLP, many of which have yet to be explored in full.

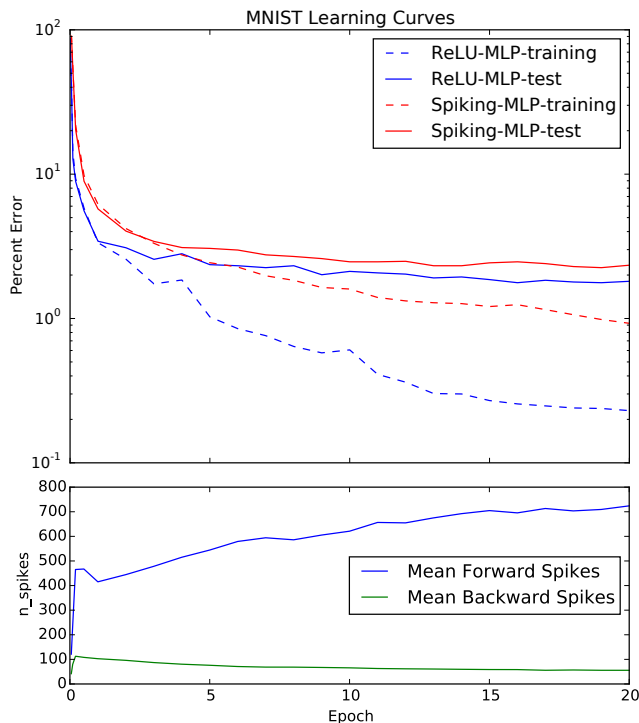


Figure 5: Top: The Learning curves of the ReLU network (blue) and the Spiking network (red). Solid lines indicate training score and dashed lines indicate test score. Bottom: The mean number of spike emitted per training iteration on the forwards (blue) and backwards (green) passes between periods at various times throughout training.

Our algorithm requires neither multiplication nor floating-point numbers to work. If we use Fractional Stochastic Gradient Descent, and scale all parameters in the network (initial weights, thresholds, and the learning rate) by the inverse of the learning rate, the only operations used are integer addition, indexing, and comparison. This makes our system very amenable to efficient hardware implementation.

Rather than arrays of floats, our network processes streams of events. This comes with some significant advantages when dealing with real-time systems. Take for example the problem of topic modeling. Rather than having to wait until the end of the sentence to receive a bag-of-words vector, we can feed in words one-by-one to the network, and sequentially build an estimate of the topic. This kind of processing allows us to react to data as soon as it comes into the network. This property, which we refer to as “low latency” could be very useful in robotics applications, where a robot is constantly required to make decisions and refine its motor signals based on the latest incoming data.

Mobile robots are usually equipped with a variety of sen-

sors operating at different rates: A gyroscope may send signals at 1000Hz while a camera will send them at 24Hz. Event based sensors may even send signals at varying rates depending on the input signals that come in. Such systems are awkward to integrate with conventional deep networks - the problem may be approached by accumulating signal statistics over time and representing them as a vector before doing an update of the entire network, but there is a necessary loss in temporal precision. Our Spiking network has no such constraints - data can simply be fed into the network when it arrives - if it is important enough to affect the output of the network, it will cause other units to fire and the signal will quickly propagate to the output of the network.

In future work, we’d like to extend our approach to more complex models. Since our model is naturally suited to temporal data, it makes sense to explore how we apply these methods to develop event-based recurrent networks. Multi-layer Perceptrons can also serve as building blocks for Variational Autoencoders (Kingma and Welling, 2013), which learn to represent the state of the world in terms of abstract, stochastic latent variables. It would be interesting to develop an event-based Variational Autoencoder for robotics applications, which learns and maintains a probabilistic latent-variable model of the world around it. Such a compact, up to date latent representation of the state of a robot’s surroundings could serve as very useful inputs for control-policy learning.

Finally, the Spiking MLP brings us one step closer to making a connection between the types of neural networks we observe in biology and the type we use in deep learning. Like biological neurons, our units maintain an internal potential, and only communicate when this potential crosses some firing threshold. In the absence of stimulating input, they are silent, and so their energy use depends on the contents of the data coming into the network. There is much research to be done on understating the relationship between the types of networks we use in deep learning and biological neural networks. Recently, (Bengio et al., 2015) showed that STDP, a neural learning rule observed in biological neurons, appears to be the following the gradient of an objective function which aims to predict the future state of the network.

Neurologists will note that our model has a major shortcoming when it comes to biological realism: we depend on bi-directional synapses and signed-spikes, neither of which are observed in biology. However (Lee et al., 2015) has recently shown that a technique called Difference Target Propagation, which depends on neither of these heresies, can serve a very similar role to backpropagation.

We believe that by building on the methods in this paper, we can bring deep learning into real-world applications.



## References

- Yoshua Bengio, Thomas Mesnard, Asja Fischer, Saizheng Zhang, and Yuhai Wu. An objective function for stdp. *arXiv preprint arXiv:1509.05936*, 2015.
- Sander M Bohte, Joost N Kok, and Johannes A La Poutré. Spikeprop: backpropagation for networks of spiking neurons. In *ESANN*, pages 419–424, 2000.
- Lars Buesing, Johannes Bill, Bernhard Nessler, and Wolfgang Maass. Neural dynamics as sampling: a model for stochastic computation in recurrent networks of spiking neurons. *PLoS Comput Biol*, 7(11):e1002211, 2011.
- Vincent Chan, Shih-Chii Liu, and André Van Schaik. Aer ear: A matched silicon cochlea pair with address event representation interface. *Circuits and Systems I: Regular Papers, IEEE Transactions on*, 54(1):48–59, 2007.
- Peter U Diehl, Daniel Neil, Jonathan Binas, Matthew Cook, Shih-Chii Liu, and Michael Pfeiffer. Fast-classifying, high-accuracy spiking deep networks through weight and threshold balancing.
- Xiequan Fan, Ion Grama, and Quansheng Liu. Hoeffding’s inequality for supermartingales. *Stochastic Processes and their Applications*, 122(10):3545–3559, 2012.
- Eric Hunsberger and Chris Eliasmith. Spiking deep networks with lif neurons. *arXiv preprint arXiv:1510.08829*, 2015.
- Diederik P Kingma and Max Welling. Auto-encoding variational bayes. *arXiv preprint arXiv:1312.6114*, 2013.
- Dong-Hyun Lee, Saizheng Zhang, Asja Fischer, and Yoshua Bengio. Difference target propagation. In *Machine Learning and Knowledge Discovery in Databases*, pages 498–515. Springer, 2015.
- Patrick Lichtsteiner, Christoph Posch, and Tobi Delbruck. A  $128 \times 128$  120 db 15  $\mu$ s latency asynchronous temporal contrast vision sensor. *Solid-State Circuits, IEEE Journal of*, 43(2):566–576, 2008.
- Emre Neftci, Srinjoy Das, Bruno Pedroni, Kenneth Kreutz-Delgado, and Gert Cauwenberghs. Event-driven contrastive divergence for spiking neuromorphic systems. *Frontiers in neuroscience*, 7, 2013.
- Peter O’Connor, Daniel Neil, Shih-Chii Liu, Tobi Delbruck, and Michael Pfeiffer. Real-time classification and sensor fusion with a spiking deep belief network. *Frontiers in neuroscience*, 7, 2013.
- Max Welling. Herding dynamical weights to learn. In *Proceedings of the 26th Annual International Conference on Machine Learning*, pages 1121–1128. ACM, 2009.

## A. Algorithms

---

### Algorithm 3 Stochastic Sampling of events from a vector

---

```

1: Input: vector  $v$ , int  $T$ 
2:  $mag \leftarrow \text{sum}(\text{abs}(\vec{v}))$ 
3:  $\vec{p} = \text{abs}(\vec{v})/mag$ 
4: for  $t \in 1 \dots T$  do
5:    $N = \text{poisson}(mag)$ 
6:   for  $n \in 1 \dots N$  do
7:      $i \leftarrow \text{DrawSample}(\vec{p})$ 
8:      $s \leftarrow \text{sign}(v_i)$ 
9:     FireSignedSpike(index =  $i$ , sign =  $s$ )

```

---



---

### Algorithm 4 Drawing a sequence of signed-spikes from a stream of vectors.

---

```

1: Input: List $_i$  Vector $_i$  stream
2:  $events \leftarrow \text{EmptyList}()$ 
3: for  $\vec{v}_t \in \text{stream}$  do
4:    $\vec{\phi} \leftarrow \vec{\phi} + \vec{v}_t$ 
5:   while True do
6:      $i \leftarrow \text{argmax}(|\vec{\phi}|)$ 
7:     if  $|\vec{\phi}_i| > \frac{1}{2}$  then
8:        $s \leftarrow \text{sign}(\vec{\phi}_i)$ 
9:        $\vec{\phi}_i \leftarrow \vec{\phi}_i - 1$ 
10:      FireSignedSpike(index= $i$ , sign= $s$ )
11:    else
12:      break

```

---

## B. Experimental Hyper-parameters

| Breadth-First                       | Depth-First    |
|-------------------------------------|----------------|
| Number of hidden layers             | 2              |
| Number of hidden units              | [200, 200]     |
| Cost function for ReLU network      | MSE            |
| Minibatch-Size                      | 1              |
| Learning rate                       | 0.01           |
| Initial weight mean magnitude       | 0.01           |
| Spiking Net Routing Scheme          | Breadth-First  |
| Optimization method                 | Fractional-SGD |
| Number of time-steps per data point | 10             |

Table 3: Hyperparameter settings for the MNIST experiment in Table 2.

## C. Event Routing

Since each event can result in a variable number of downstream events, we have to think about the order in which we want to process these events. There are two issues:

1. In situations where one event is sent to multiple modules, we need to ensure that it is being sent to its downstream modules in the right order. In the case of the SMLP, we need to ensure that, for a given input, its child-events reach the filters in the backward pass before its other child-events make their way around and do the backward pass. Otherwise we are not implementing backpropagation correctly.
2. In situations where one event results in multiple child-events, we need to decide in which order to process these child events and their child events. For this, there are two routing schemes that we can use: Breadth-first and depth-first. We will outline those with the example shown in Figure 6. Here we have a module  $A$  that responds to some input event by generating two events:  $a_1$  and  $a_2$ . Event  $a_1$  is sent to module  $B$  and triggers events  $b_1$  and  $b_2$ . Event  $a_2$  is sent and triggers event  $b_3$ . Table 4 shows how a breadth-first vs depth-first router will handle these events.

| Breadth-First | Depth-First |
|---------------|-------------|
| $B(a_1)$      | $B(a_1)$    |
| $B(a_2)$      | $D(b_1)$    |
| $C(a_1)$      | $D(b_2)$    |
| $C(a_2)$      | $C(a_1)$    |
| $D(b_1)$      | $B(a_2)$    |
| $D(b_2)$      | $D(b_3)$    |
| $D(b_3)$      | $C(a_2)$    |

Table 4: Depth-First and Breadth-First routing differ in their order of event processing. This table shows the order of event processed in each scheme. Refer to 6.

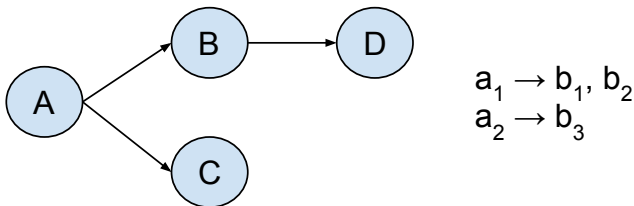


Figure 6: A simple graph showing 4 modules. Module  $A$  generates an event  $a_1$  that causes two events:  $b_1$  and  $b_2$ . These are then distributed to downstream modules. The order in which events are processed depends on the routing scheme.

Experimentally, we found that Breadth-First routing performed better on our MNIST task, but we should keep an open mind on both methods until we understand why.

## D. Code

Code for this project was written in Python and Java. The source code to replicate any of these projects can be found in our public git repository at:

[github.com/petered/spiking-mlp](https://github.com/petered/spiking-mlp)